

Supporting Information

2-Hydroxy-3-methoxybenzylidene thiosemicarbazide (H_2L^1). White powder. Yield = 71 %. 1H -NMR (DMSO- d_6 , 25 °C), δ : 3.80 (s, 3H, OCH₃), 6.77 (t, 1H; J = 7.9 Hz, ArH), 6.96 (d, 1H, J = 7.8 Hz, ArH), 7.52 (d, 1H, J = 7.8 Hz, ArH), 7.87 (s, br, 1H, NH), 8.09 (s, br, 1H, NH), 8.40 (s, 1H; HC=N), 9.20 (s, br, 1H, OH), 11.39 (s, br, 1H; NH). ESI-MS (positive ions, m/z) = 225.0 ($[M]^+$, 100); IR (ATR, cm^{-1}): ν_{NH} = 3459, 3339; ν_{OH} = 3158 (br); $\nu_{C=N}$ = 1596; $\nu_{C=S}$ = 1532, 821; ν_{OCH_3} = 1258, 1056. Anal. Calcd. for $C_9H_{11}N_3O_2S \cdot 0.5H_2O$: C 46.14; H 5.16; N 17.94. Found: C 45.92, H 4.82, N 18.24.

2-hydroxy-3-methoxybenzaldehyde-4-ethyl-3-thiosemicarbazone (H_2L^2). White powder. Yield = 85%. 1H -NMR (DMSO- d_6 , 25°C), δ : 1.13 (t, 3H, CH_2CH_3); 3.58 (q, 2H, CH_2CH_3); 3.81 (s, 3H, OCH₃); 6.78 (t, 1H, ArH, J = 7.9); 6.96 (d, 1H, ArH, J = 6.6); 7.54 (d, 1H, ArH, J = 7.3); 8.39 (s, 1H, CH=N); 8.44 (s, br, 1H, NH); 9.20 (s, br, 1H, OH); 11.38 (s, 1H, NH). ESI-MS (positive ions, m/z) = 253.1 ($[M]^+$, 100). IR (ATR, cm^{-1}): ν_{NH} = 3305; $\nu_{C=N}$ = 1522; $\nu_{C=S}$ = 1063, 784. Anal. Calcd. for $C_{11}H_{15}N_3O_2S \cdot H_2O$: C 48.69, H 6.13, N 15.49, S 11.82. Found: 48.66, H 6.25, N 15.54, S 12.01.

2-hydroxy-3-methoxybenzylidene semicarbazone (H_2L^3). Yield = 81%. 1H -NMR (DMSO- d_6 , 25°C), δ : 3.84 (s, 3H, OCH₃), 6.39 (s, br, 2H, NH₂), 6.76 (t, J = 7.8 Hz, 1H, ArH), 6.92 (d, J = 7.6 Hz, 1H, ArH), 7.37 (d, 1H; J = 7.8, ArH), 8.17 (s, 1H; HC=N), 9.20 (s, br, 1H; OH), 10.20 (s, br, 1H; NH). ESI-MS (positive ions, m/z) = 209.2 ($[M]^+$, 100); IR (ATR; cm^{-1}): ν_{NH} = 3466; ν_{OH} = 3170-3280 (br); $\nu_{C=O}$ = 1672; $\nu_{C=N}$ = 1586. Anal. Calcd for $C_9H_{11}N_3O_3 \cdot 1/4H_2O$: C 50.58; H 5.42; N 19.66. Found: C 50.67; H 5.37; N 19.44.

Sodium 2-hydroxy-3-methoxy-5-sulfonate-benzaldehyde-3-thiosemicarbazone (NaH_2L^4). Beige powder. Yield = 53%. 1H NMR (DMSO- d_6 , 25°C), δ : 11.41 (b, 1H, NH), 9.38 (b, 1H, OH), 8.40 (s, 1H, CH=N), 8.11 (b, 1H, NH), 7.71 (b, 1H, NH), 7.60 (d, J = 1.9 Hz, 1H, ArH), 7.16 (d, J = 1.9 Hz, 1H, ArH), 3.81 (s, 3H, OCH₃). ^{13}C NMR (101 MHz, DMSO- d_6 , 25°C), δ : 177.7, 146.9, 146.2, 140.5, 139.7, 119.1, 115.6, 110.4, 55.9. ESI-MS (negative ions, m/z): 304.3 ($(M-Na)^-$). IR (ATR, cm^{-1}): $\nu_{NH_2} + \nu_{OH}$ = 3384; ν_{NH} =

3173; $\nu_{\text{C}=\text{N}} = 1609$; $\nu_{\text{C}=\text{S}} = 1257$; $\nu_{\text{SO}_3} = 1104, 1038$. Anal. Calcd for $\text{C}_9\text{H}_{10}\text{N}_3\text{NaO}_5\text{S}_2 \cdot \text{H}_2\text{O}$: C 31.30, H 3.50, N 12.17, S 18.57. Found: C 31.56, H 3.17, N 12.17, S 18.98.

Sodium 2-hydroxy-3-methoxy-5-sulfonate-benzaldehyde-4-ethyl-3-thiosemicarbazone (NaH_2L^5). White powder. Yield = 57%. ^1H NMR (DMSO-d_6 , 25°C), δ : 11.35 (s, 1H, NH), 9.37 (b, 1H, OH), 8.41 (s, 1H, $\text{CH}=\text{N}$), 8.33 (t, $J = 6.0$ Hz, 1H, NH), 7.63 (d, $J = 1.9$ Hz, 1H, ArH), 7.17 (d, $J = 1.9$ Hz, 1H, ArH), 3.81 (s, 3H, OCH_3), 3.58 (p, $J = 6.9$ Hz, 2H, CH_2), 1.14 (t, $J = 7.1$ Hz, 3H, CH_3). ^{13}C NMR (101 MHz, DMSO-d_6 , 25°C), δ : 176.5, 146.8, 146.1, 140.0, 139.6, 119.4, 115.6, 110.4, 55.9, 18.6, 14.7. ESI-MS (negative ions, m/z): 332.2 ($\text{M}-\text{Na}$) $^-$. IR (ATR, cm^{-1}): $\nu_{\text{OH}} = 3384$; $\nu_{\text{NH}} = 3173$; $\nu_{\text{C}=\text{N}} = 1609$; $\nu_{\text{C}=\text{S}} = 1257$; $\nu_{\text{SO}_3} = 1104, 1038$. Anal. Calcd for $\text{C}_{11}\text{H}_{14}\text{N}_3\text{S}_2\text{O}_5\text{Na}$: C 37.17, H 3.97, N 11.82, S 18.05. Found: C 37.08, H 4.30, N 11.19, S 18.11.

General synthesis for complexes 1, 4, 5, 8, 9. 0.15 g of the ligand were dissolved in methanol and the pH was adjusted to 8-9 by adding NaOH 1M, resulting in a yellow solution. An equimolar amount of $\text{CuCl}_2 \cdot 2\text{H}_2\text{O}$ in methanol was added and a dark green precipitate appeared. The suspension was stirred for 4 hours at r.t. The solvent was partially evaporated under vacuum and the dark green powder was filtered off and washed with cold methanol.

(1), $[\text{CuL}^1\text{Cl}] \cdot 3\text{H}_2\text{O}$. Dark green powder. Yield: 52%. MS-ESI (positive ions) m/z (%) = 287 ($[\text{CuL}]^+$, 100); 345 ($[\text{CuLCl}+\text{Na}]^+$, 70). IR (ATR, cm^{-1}): $\nu_{\text{NH}} = 3280, 3168$; $\nu_{\text{C}=\text{N}+\delta\text{N}-\text{H}} = 1634, 1604$; $\nu_{\text{CS}} = 1217$. Anal. Calcd. for $\text{C}_9\text{H}_{10}\text{CuClN}_3\text{O}_2\text{S} \cdot 3\text{H}_2\text{O}$: C 28.65; H 4.27; N 11.14. Found: C 28.82; H 4.09; N 10.96.

(4), $[\text{CuL}^2\text{Cl}] \cdot 1.5 \text{H}_2\text{O}$. Dark green powder. Yield: 71%. MS-ESI (positive ions) m/z (%) = 315 ($[\text{CuL}]^+$, 100); 373 ($[\text{CuLCl}+\text{Na}]^+$, 10). IR (ATR, cm^{-1}): $\nu_{\text{NH}} = 3347, 3299$; $\nu_{\text{C}=\text{N}+\delta\text{N}-\text{H}} = 1605, 1586$; $\nu_{\text{CS}} = 1219$. Anal. Calcd. for $\text{C}_{11}\text{H}_{14}\text{N}_3\text{O}_2\text{SCuCl} \cdot 1.5 \text{H}_2\text{O}$: C 34.92, H 4.53, N 11.11. Found: C 34.84, H 3.98, N 10.87.

(8), $[\text{Cu}(\text{NaHL}^4)\text{Cl}]$. Dark green powder. Yield: 77%. MS-ESI (negative ions) m/z (%) = 365.2 ($[\text{CuL}]^-$, 100). IR (ATR, cm^{-1}): $\nu_{\text{OH}}+\nu_{\text{NH}_2} = 3433, 3317$; $\nu_{\text{C}=\text{N}} = 1650$; $\nu_{\text{C}=\text{S}} = 1248$; $\nu_{\text{SO}_3} = 1170$,

1040. Anal. Calcd. for $C_9H_9N_3NaO_5S_2CuCl$: C 25.42, H 2.13, N 9.88, S 15.08. Found: C 25.23, H 2.26, N 9.49, S 15.47.

(9), $[Cu(NaHL^5)Cl] \cdot H_2O$. Dark green powder. Yield: 90%. MS-ESI (negative ions) m/z (%) = 393.3 ($[CuL]^-$, 100); 789.0 ($([Cu(HL)]_2-H^+)^-$, 10). IR (ATR, cm^{-1}): $\nu_{NH} = 3154, 3053$; $\nu_{C=N} = 1606$; $\nu_{C=S} = 1245$; $\nu_{SO_3} = 1176, 1036$. Anal. Calcd. for $C_{11}H_{13}N_3NaO_5S_2CuCl \cdot H_2O$: C 28.03, H 3.21, N 8.91, S 13.61. Found: C 27.89, H 3.20, N 8.65, S 14.01.

Scheme S1. Synthesis of the ligands. Semicarbazide is used as chlorohydrated salt and aqueous NaOH is added in situ to obtain the neutral semicarbazide.

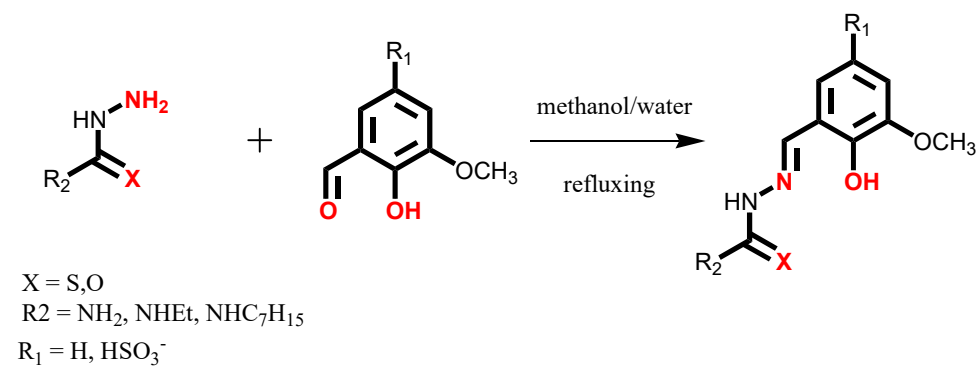
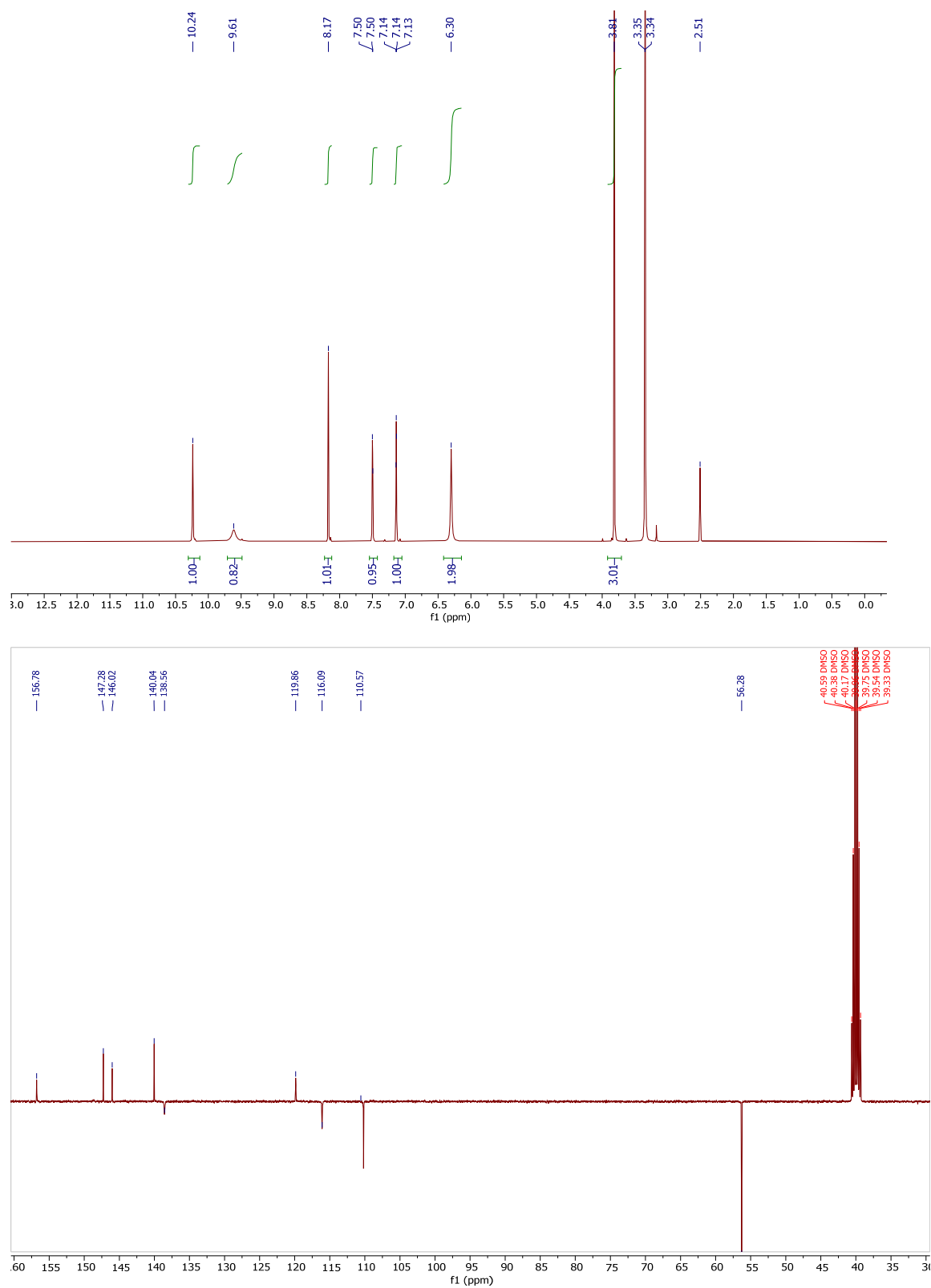
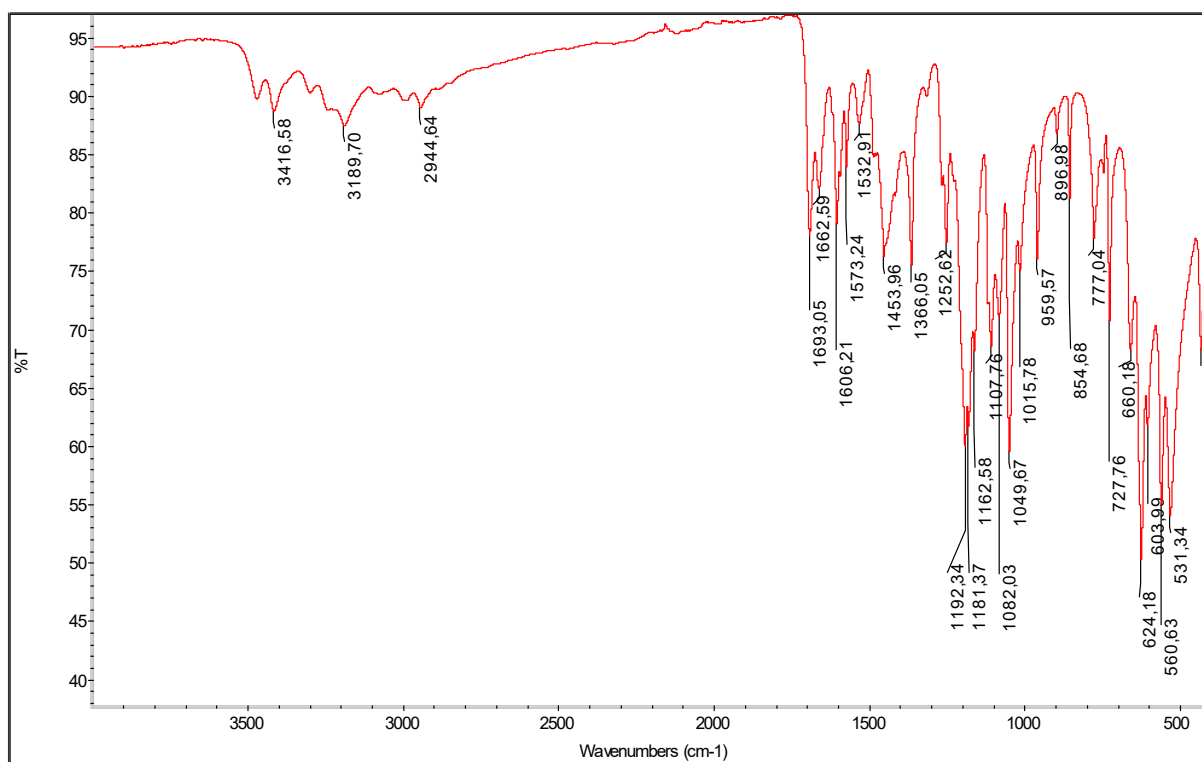


Figure S1. A) ^1H NMR (top) and ^{13}C NMR (DEPT, bottom) spectrum of $\text{NaH}_2\text{L6}$ registered in DMSO-d_6 . **B)** ATR-IR spectrum and **C)** mass spectrum (ESI-MS, negative ions) of ligand $\text{NaH}_2\text{L6}$.

A)



B)



C)

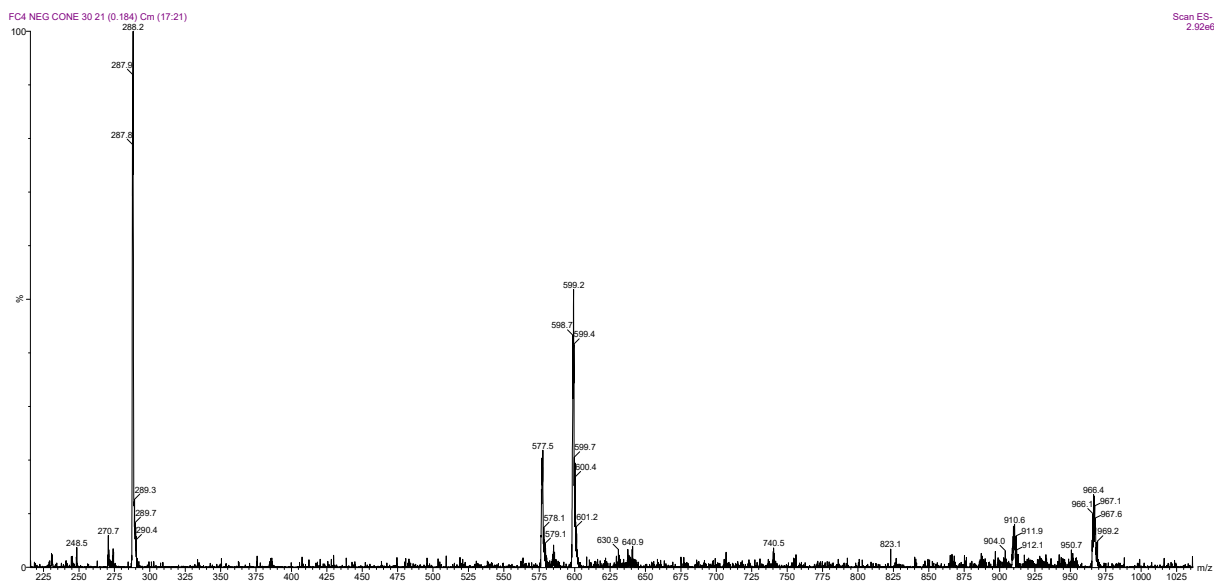
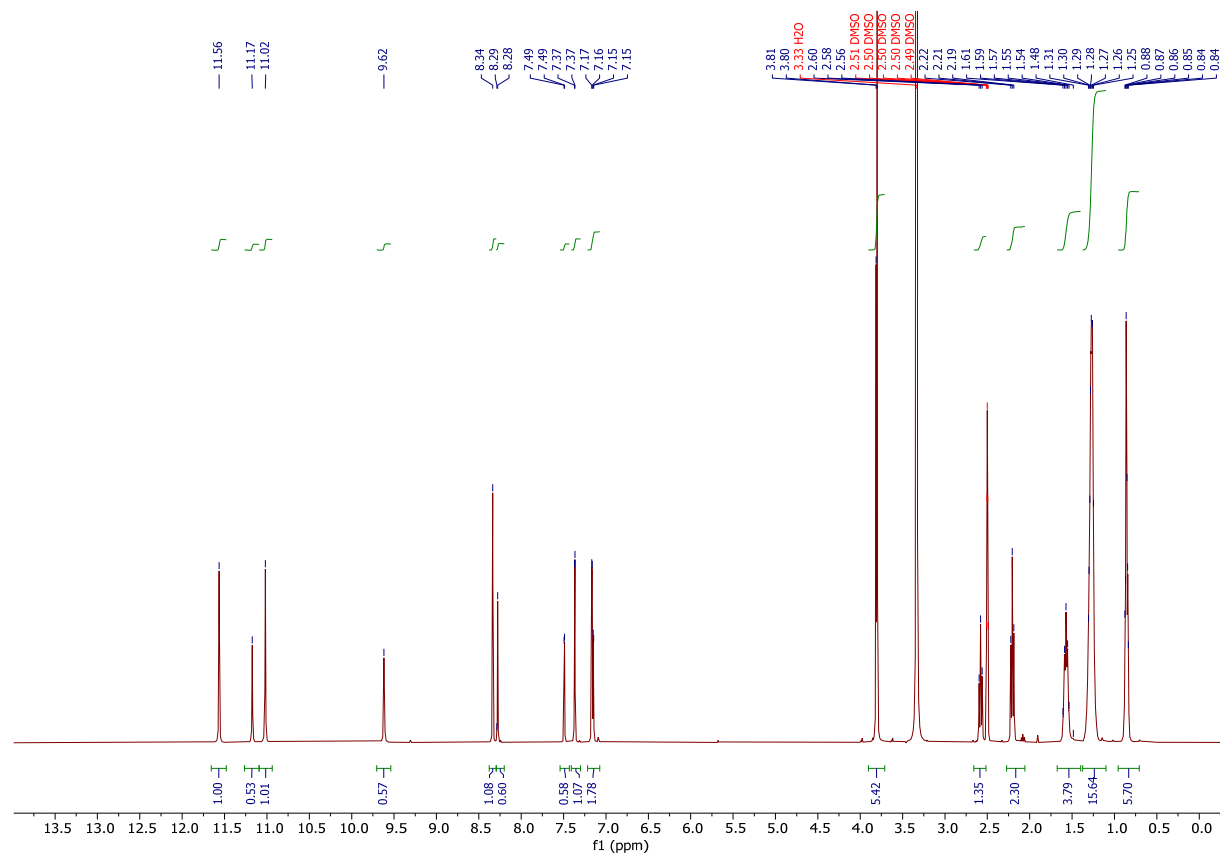
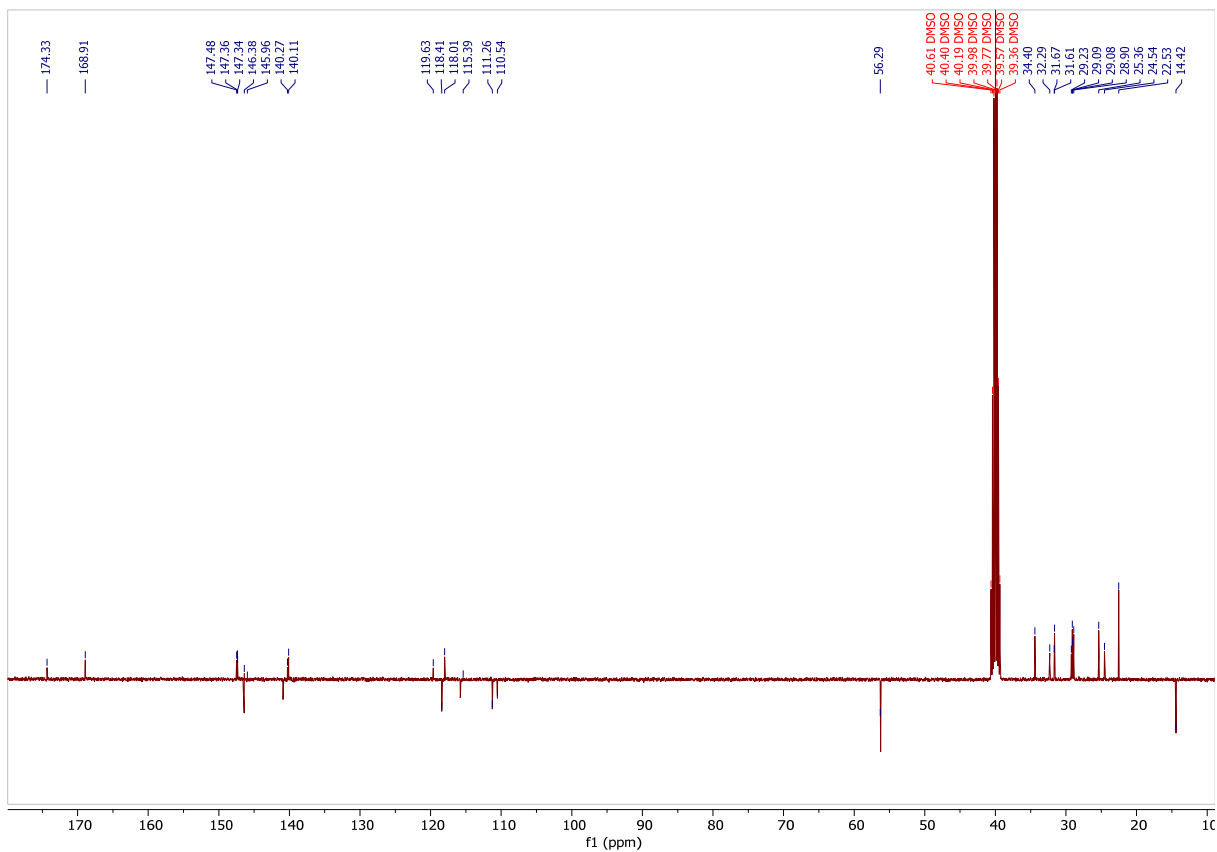


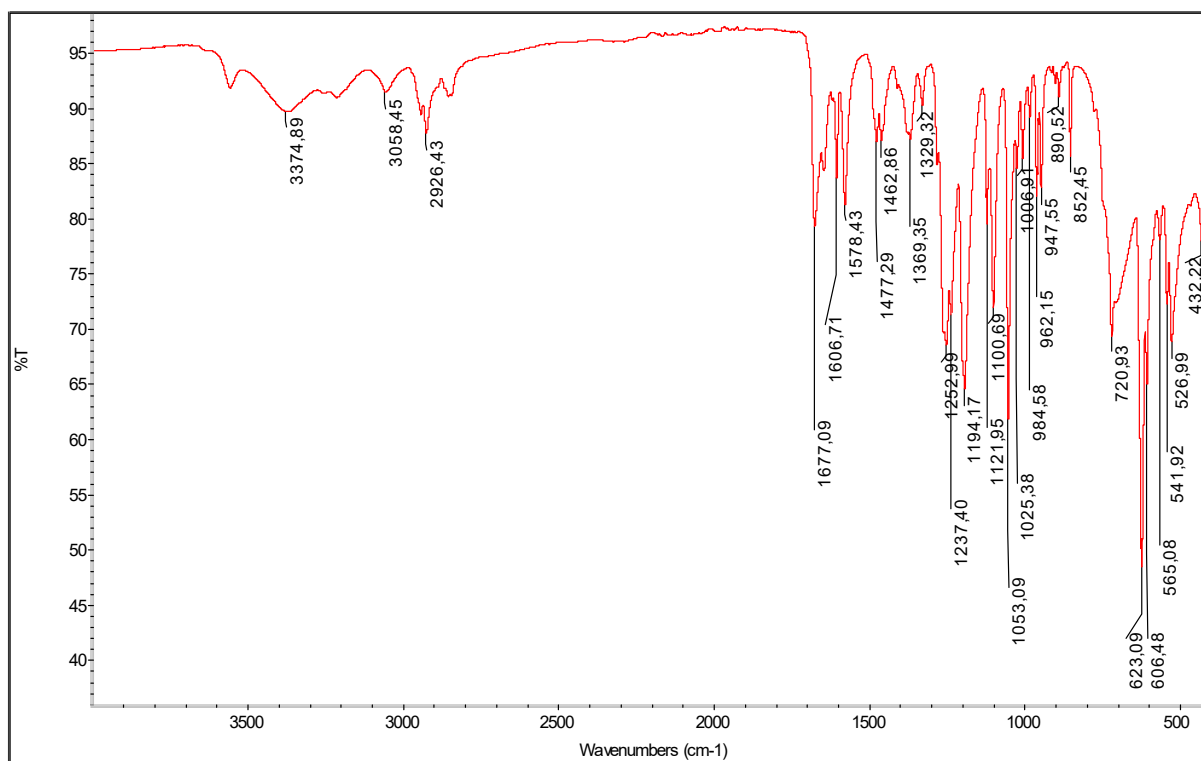
Figure S2. A) ^1H NMR (top) and ^{13}C NMR (DEPT, bottom) spectrum of $\text{NaH}_2\text{L7}$ registered in DMSO-d_6 . **B)** ATR-IR spectrum and **C)** mass spectrum (ESI-MS, negative ions) of ligand $\text{NaH}_2\text{L6}$.

A)





B)



C)

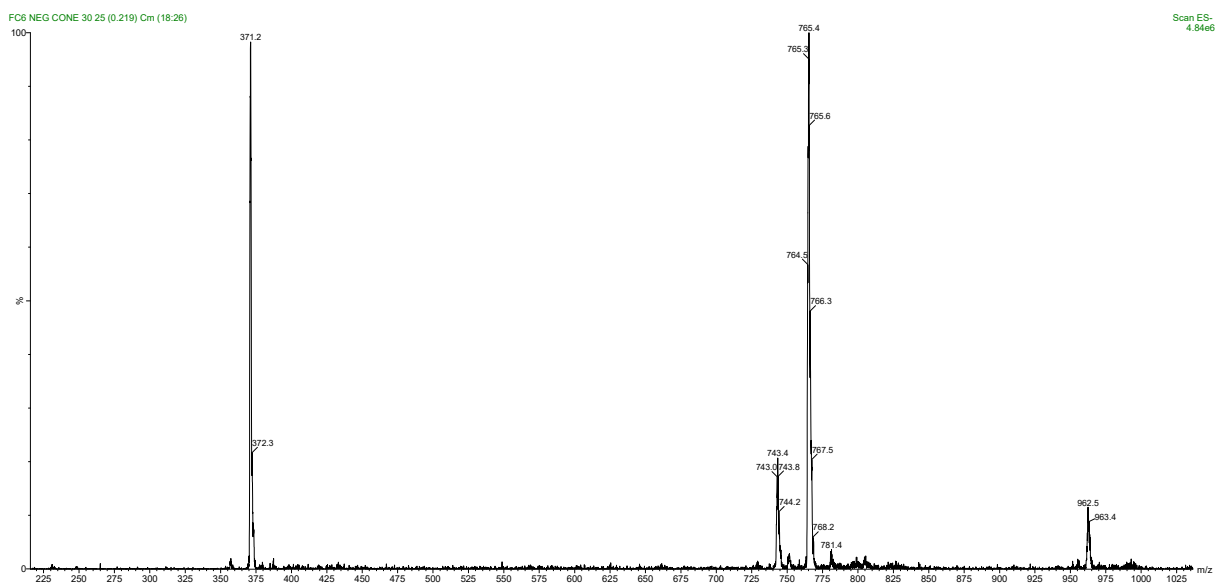


Figure S3. IR spectrum of complex **5**.

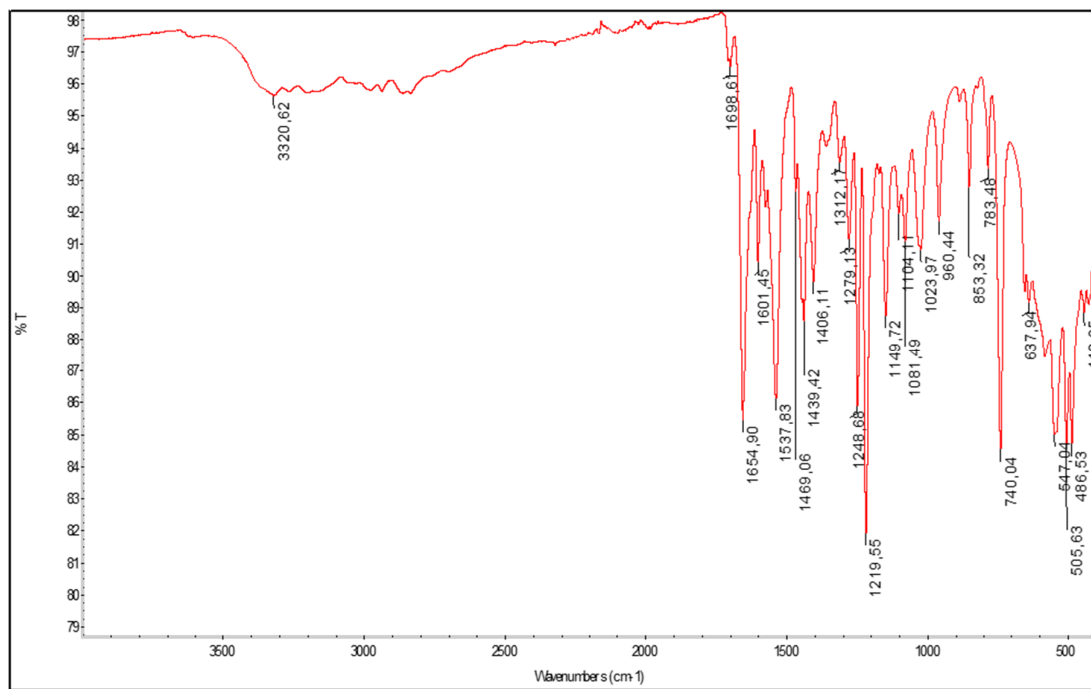


Figure S4. ESI-MS spectrum for complex **5** (negative ions, solvent: methanol).

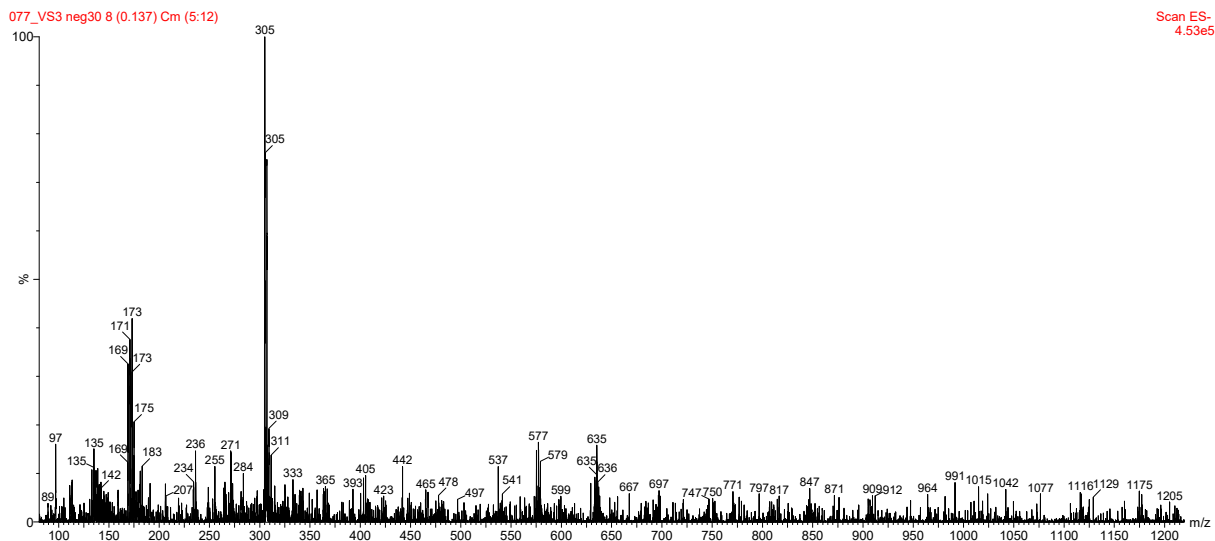


Figure S5. IR spectrum of complex **2**.

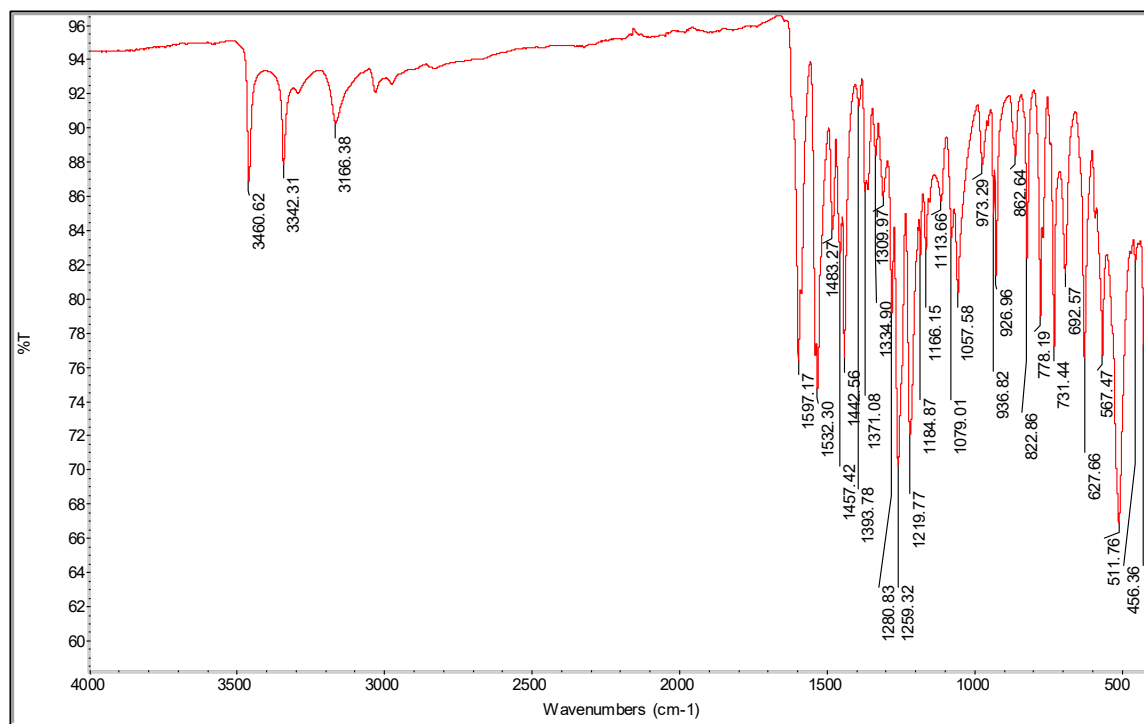


Figure S6. IR spectrum of complex **3**.

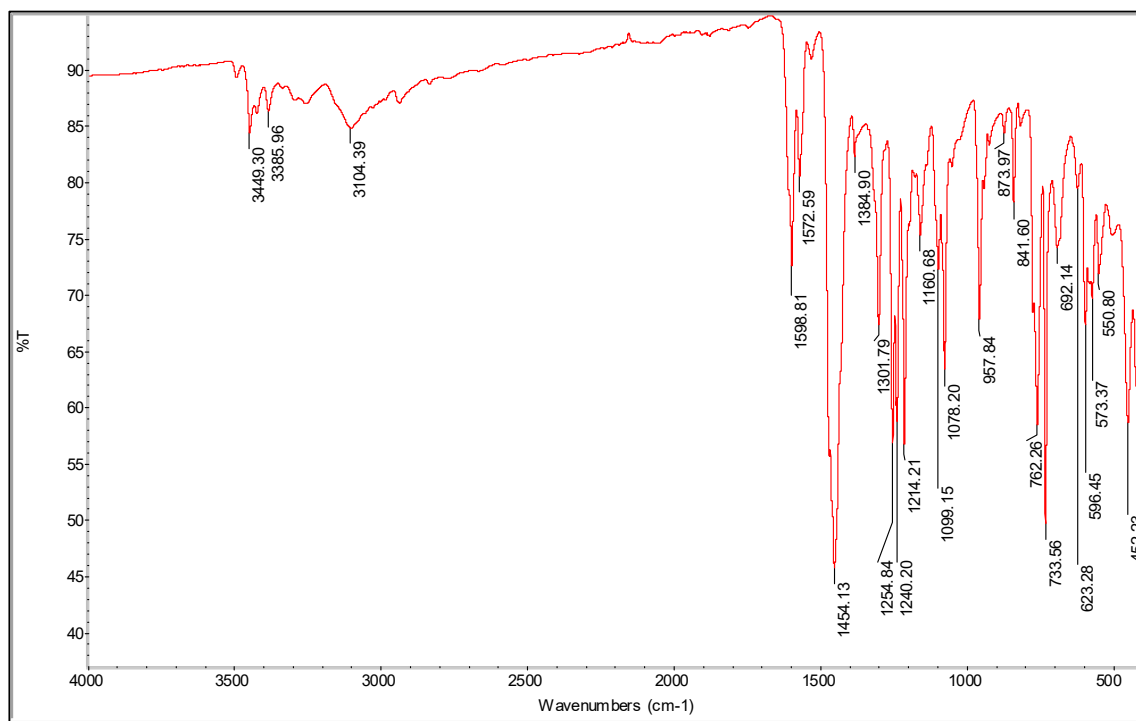


Figure S7. IR spectrum of complex **6**.

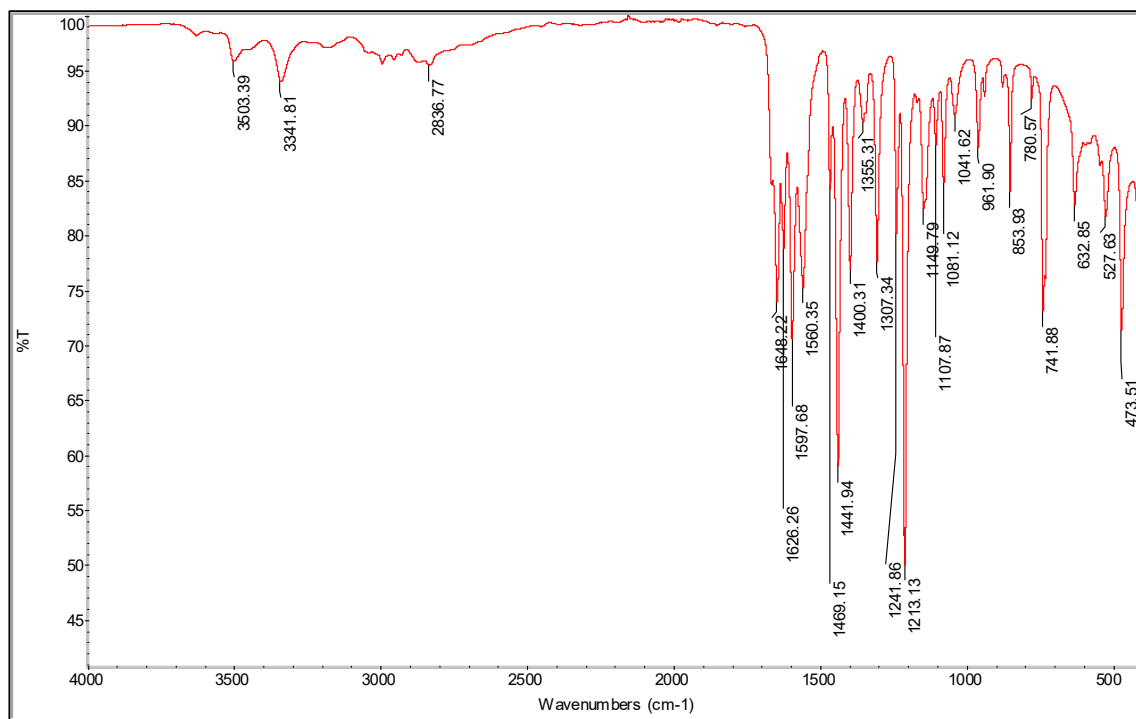


Figure S8. IR spectrum of complex **7**.

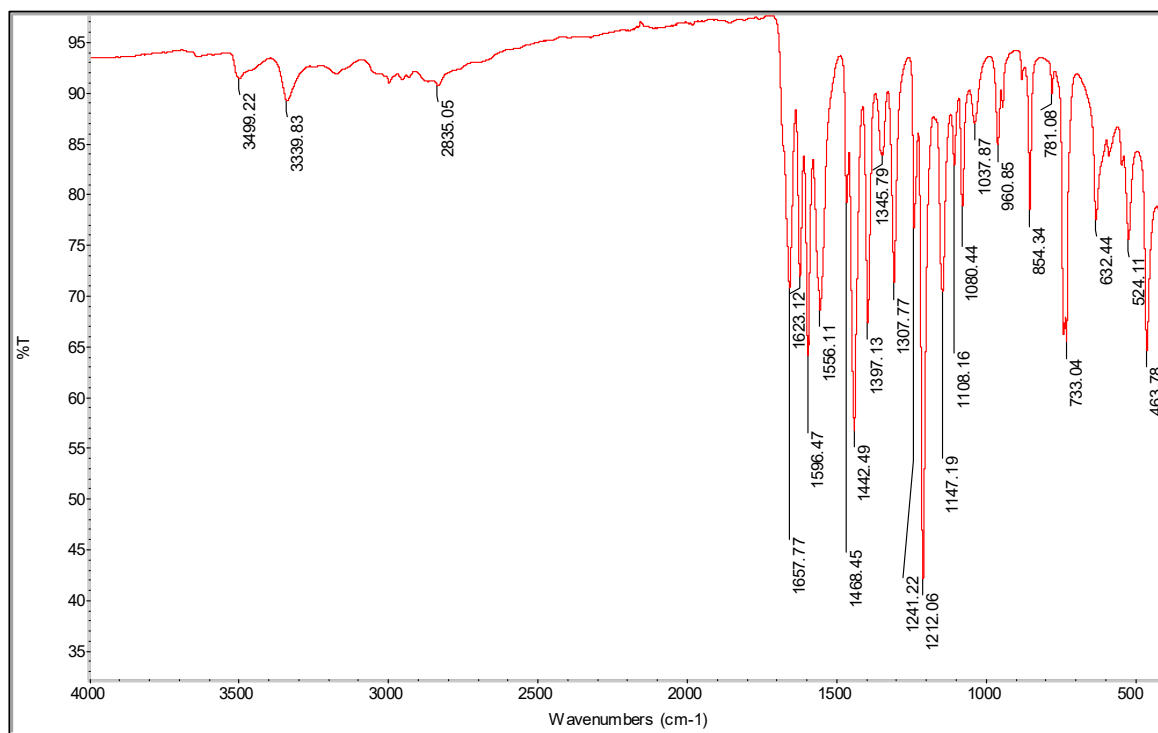
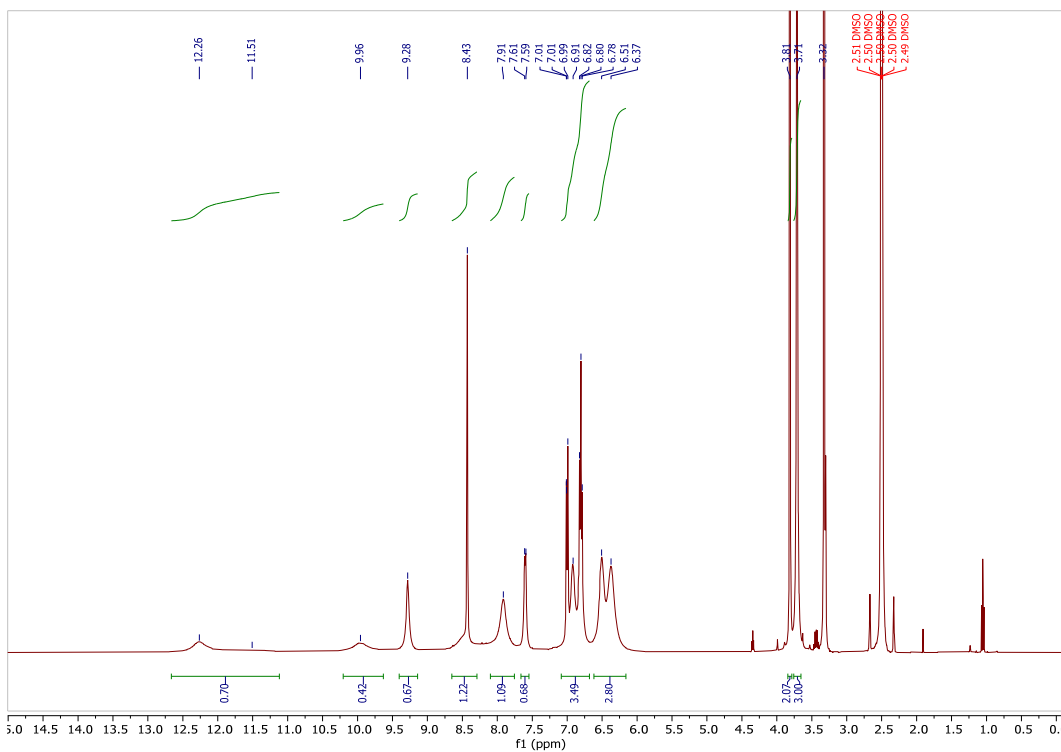


Figure S9. ^1H NMR (top) and ^{13}C NMR (bottom) spectrum of complex **2** registered in DMSO- d_6 .



VS4 13C.10.fid — ^{13}C NMR VS4 DMSO d_6 14/5/25

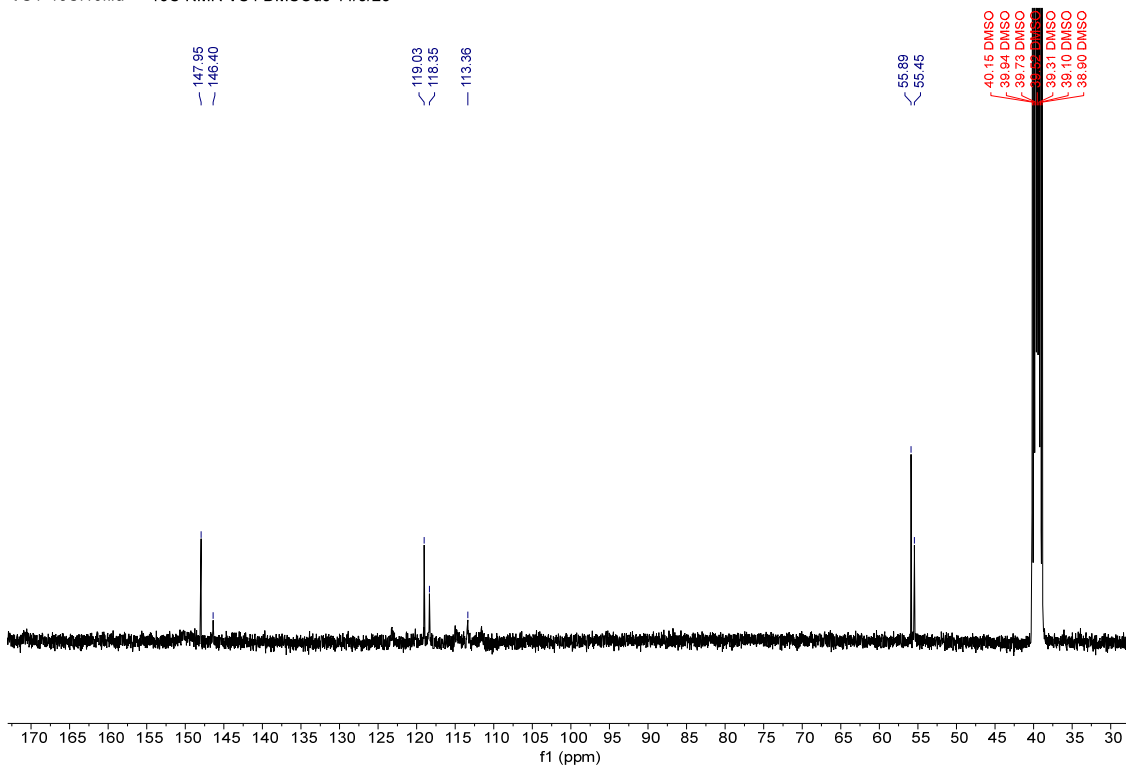


Figure S10. ^1H NMR spectrum of complex **7** registered in DMSO-d_6 .

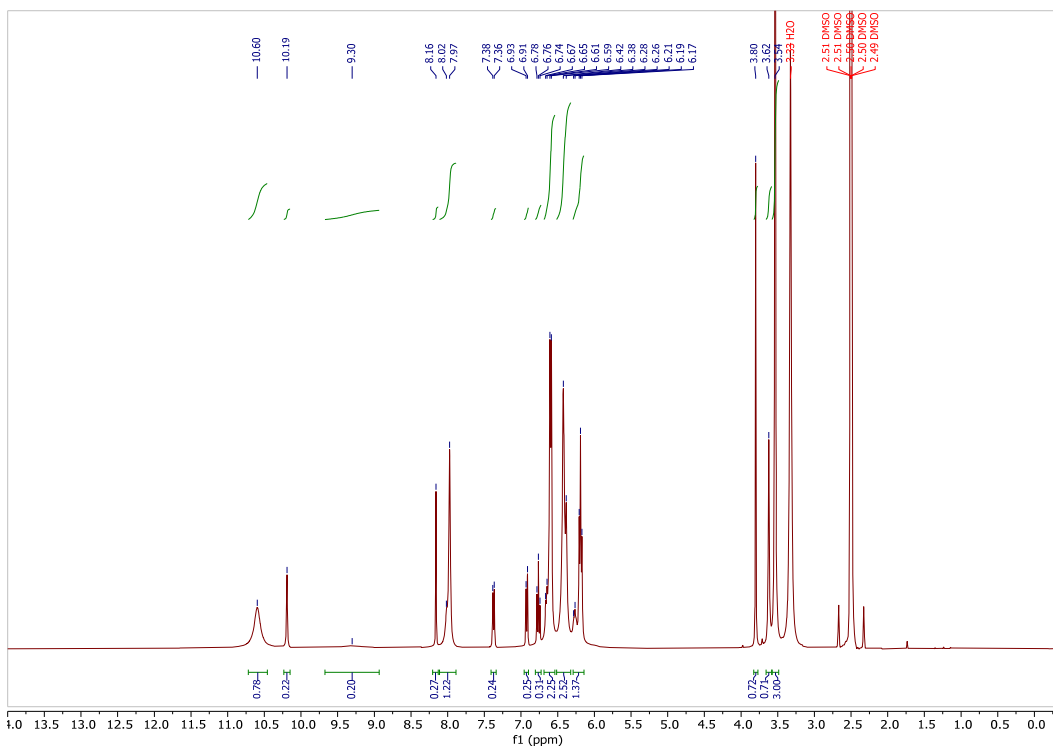


Figure S11. ^1H NMR spectrum of complex **12** registered in DMSO-d_6 .

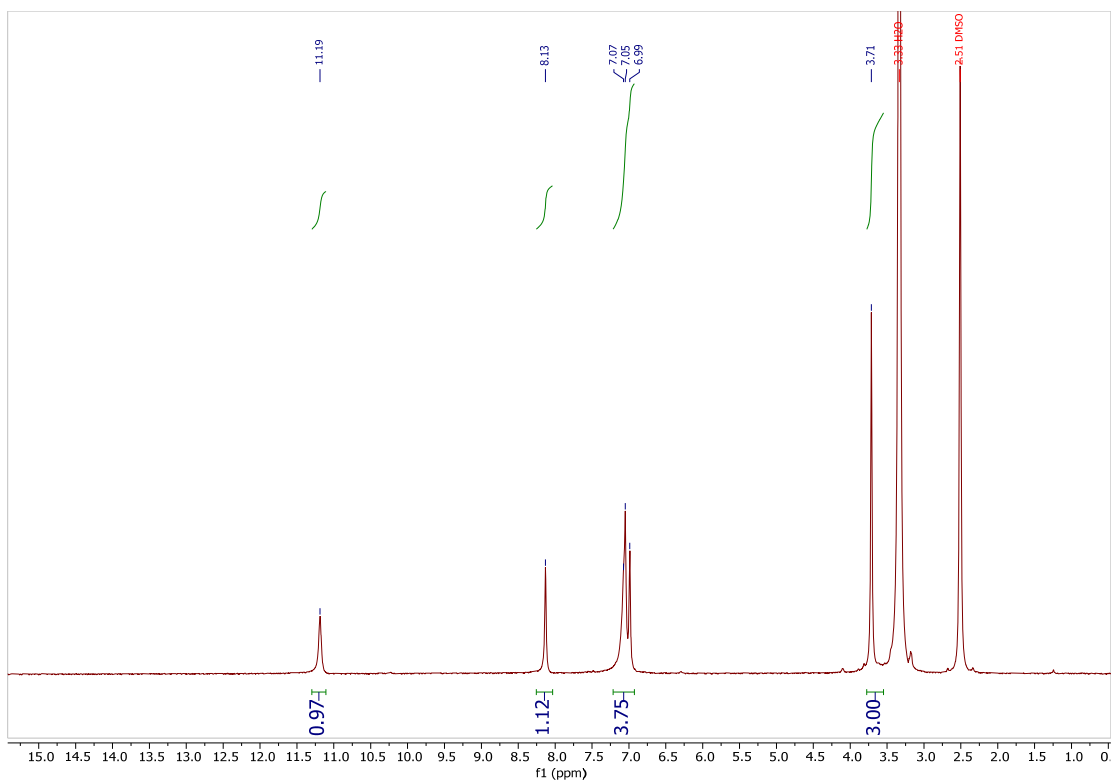


Figure S12. ^1H NMR spectrum of complex **14** registered in DMSO-d_6 .

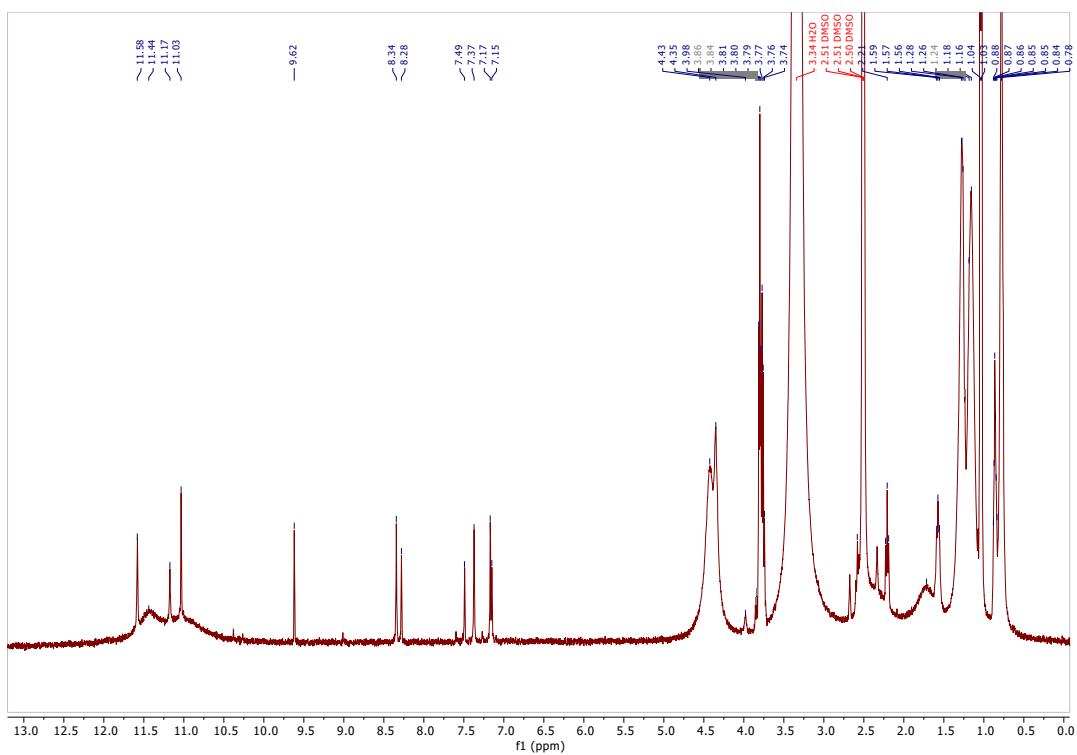


Figure S13. IR spectrum of complex **10**.

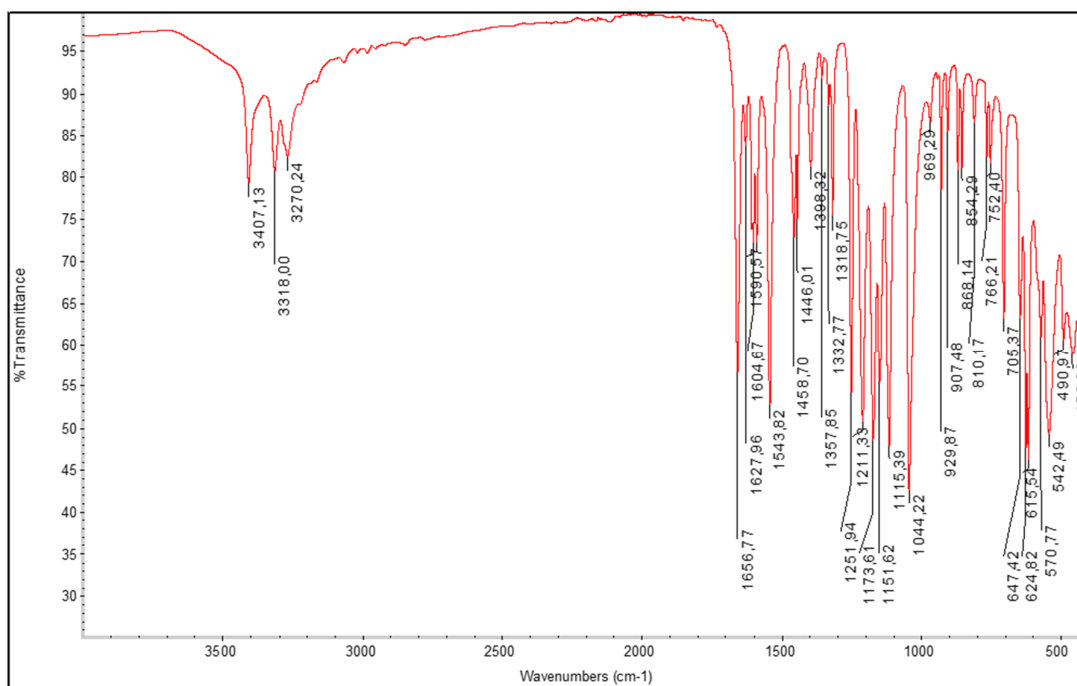


Figure S14. IR spectrum of complex **11**.

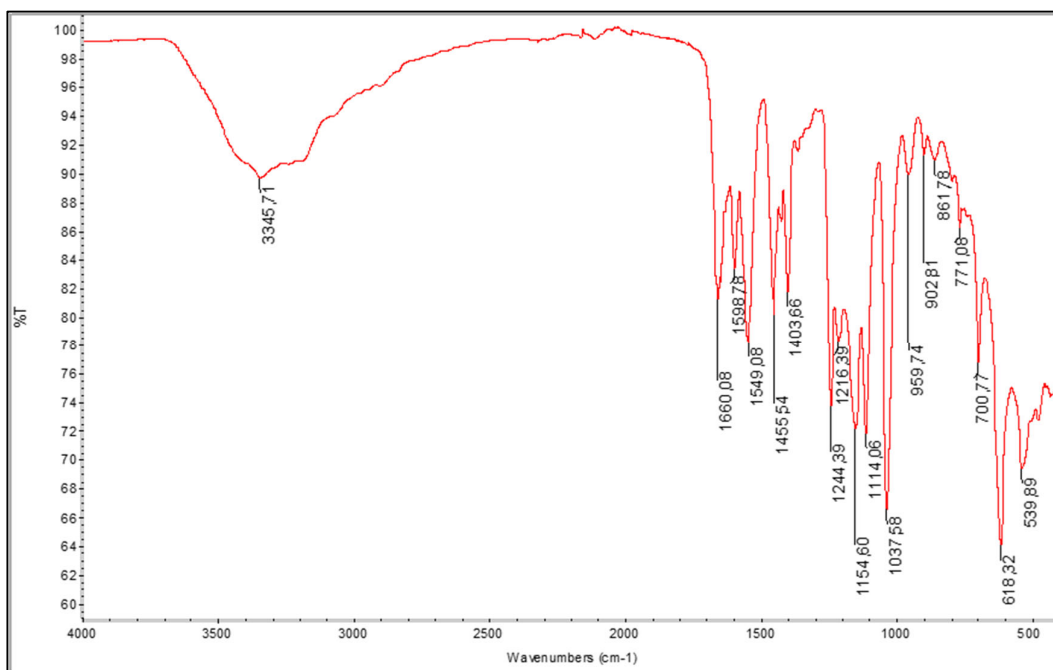


Figure S15. IR spectrum of complex **12**.

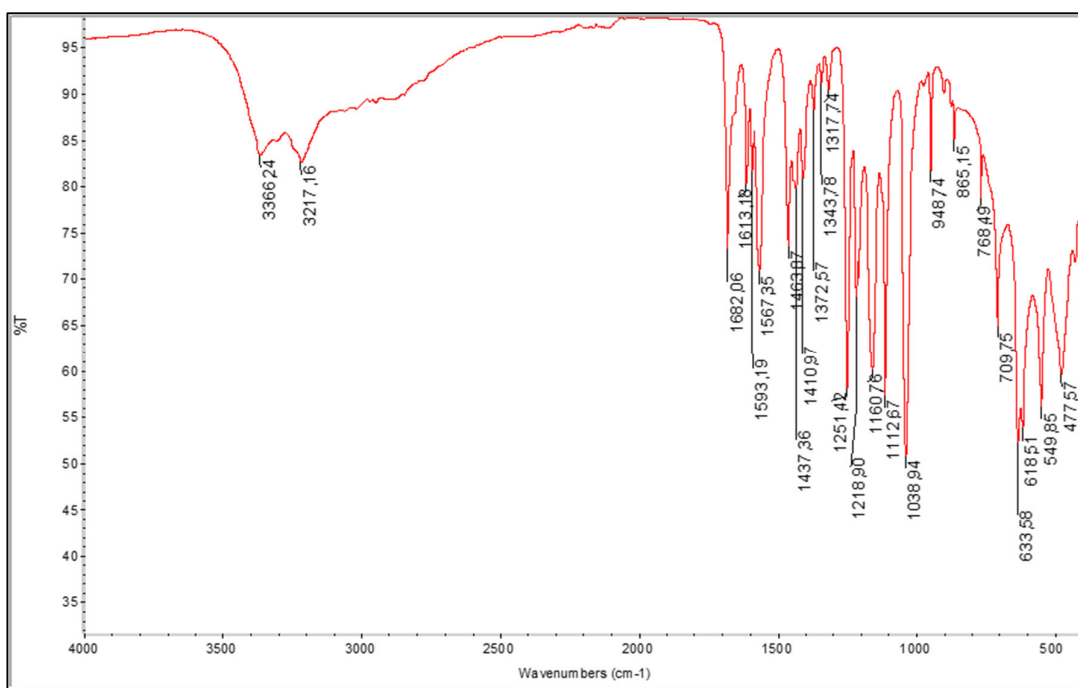


Figure S16. IR spectrum of complex **13**.

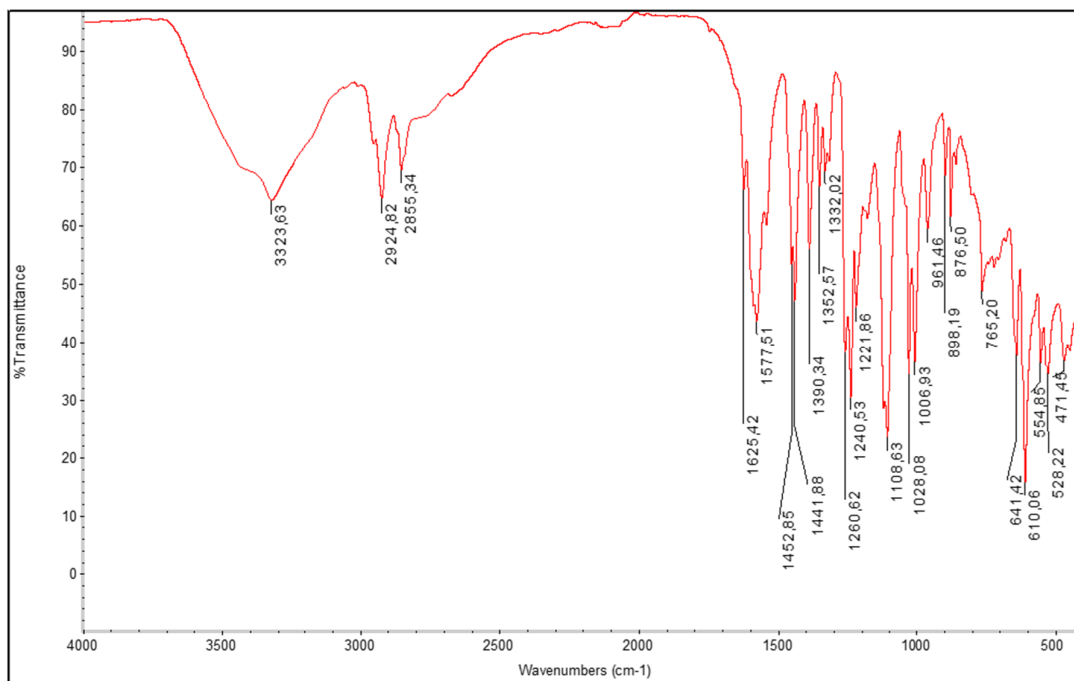


Figure S17. IR spectrum of complex **14**.

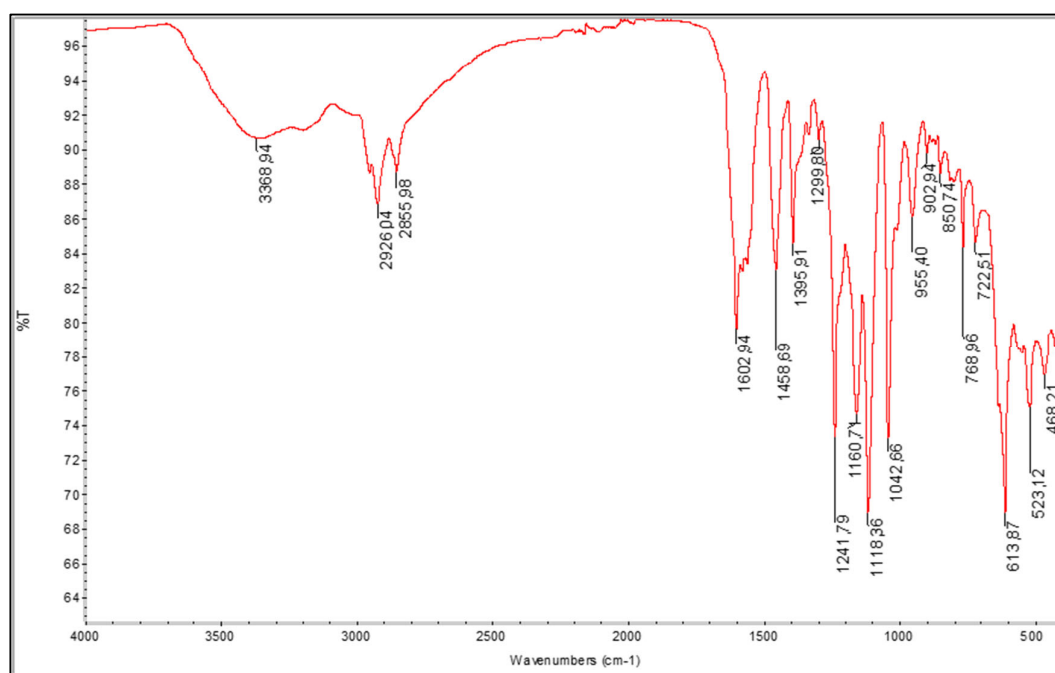
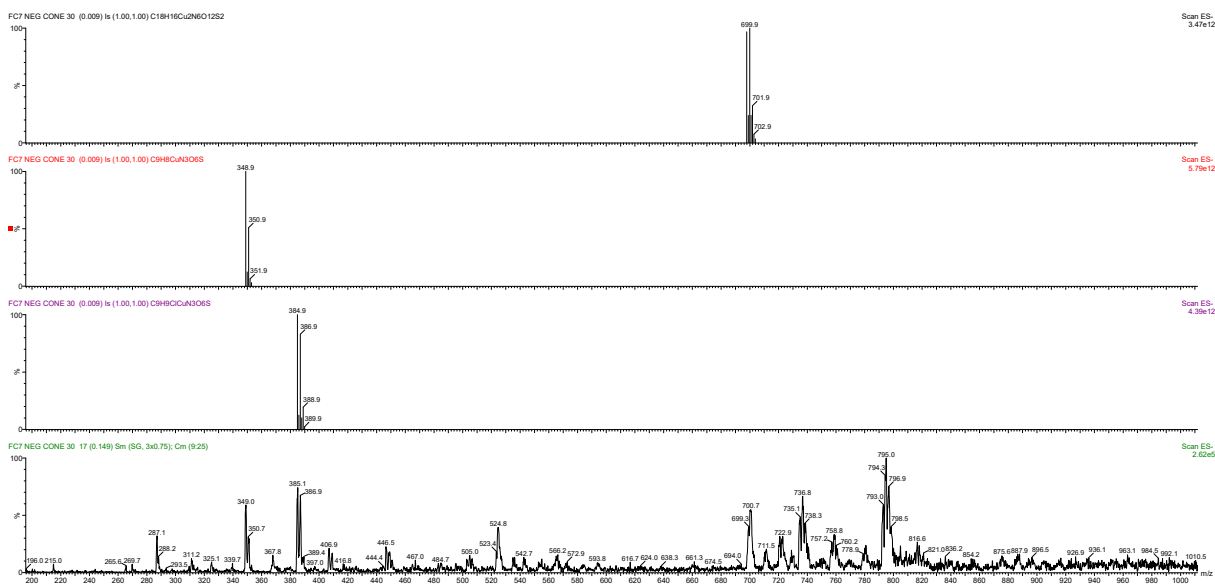


Figure S18. ESI-MS spectrum for complex **10** (negative ions; solvent: methanol).



Top plot: F09 NEG CONE 30 (0.009) Is (1.00,1.00) C12H42Cl2N4O12S2. Base peak at 867.1. Other peaks at 865.1, 868.1, 870.1, 871.1.

Middle plot: F09 NEG CONE 30 (0.009) Is (1.00,1.00) C12H42Cl2N4O12S2. Base peak at 469.0. Other peaks at 470.0, 472.0, 473.0.

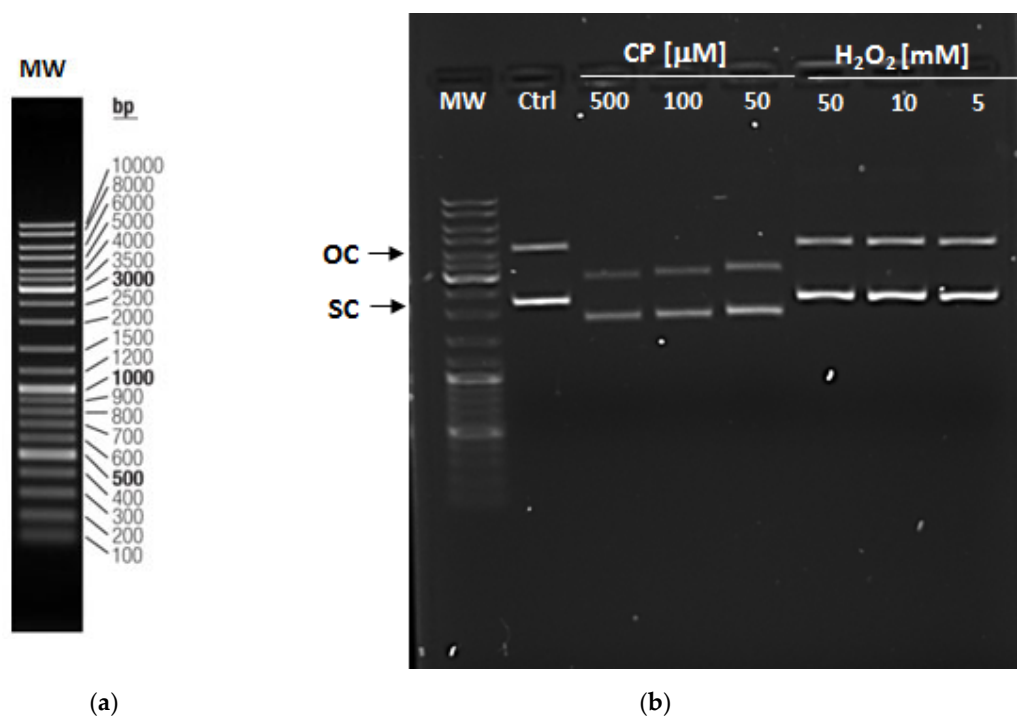
Bottom plot: F09 NEG CONE 30 16 (0.140) Cm (10.25). Base peak at 867.2. Other peaks at 432.3, 434.0, 469.0, 468.4, 471.5, 473.0, 475.0, 476.0, 477.0, 478.0, 479.0, 480.0, 481.0, 482.0, 483.0, 484.0, 485.0, 486.0, 487.0, 488.0, 489.0, 490.0, 491.0, 492.0, 493.0, 494.0, 495.0, 496.0, 497.0, 498.0, 499.0, 500.0, 501.0, 502.0, 503.0, 504.0, 505.0, 506.0, 507.0, 508.0, 509.0, 510.0, 511.0, 512.0, 513.0, 514.0, 515.0, 516.0, 517.0, 518.0, 519.0, 520.0, 521.0, 522.0, 523.0, 524.0, 525.0, 526.0, 527.0, 528.0, 529.0, 530.0, 531.0, 532.0, 533.0, 534.0, 535.0, 536.0, 537.0, 538.0, 539.0, 540.0, 541.0, 542.0, 543.0, 544.0, 545.0, 546.0, 547.0, 548.0, 549.0, 550.0, 551.0, 552.0, 553.0, 554.0, 555.0, 556.0, 557.0, 558.0, 559.0, 560.0, 561.0, 562.0, 563.0, 564.0, 565.0, 566.0, 567.0, 568.0, 569.0, 570.0, 571.0, 572.0, 573.0, 574.0, 575.0, 576.0, 577.0, 578.0, 579.0, 580.0, 581.0, 582.0, 583.0, 584.0, 585.0, 586.0, 587.0, 588.0, 589.0, 590.0, 591.0, 592.0, 593.0, 594.0, 595.0, 596.0, 597.0, 598.0, 599.0, 600.0, 601.0, 602.0, 603.0, 604.0, 605.0, 606.0, 607.0, 608.0, 609.0, 610.0, 611.0, 612.0, 613.0, 614.0, 615.0, 616.0, 617.0, 618.0, 619.0, 620.0, 621.0, 622.0, 623.0, 624.0, 625.0, 626.0, 627.0, 628.0, 629.0, 630.0, 631.0, 632.0, 633.0, 634.0, 635.0, 636.0, 637.0, 638.0, 639.0, 640.0, 641.0, 642.0, 643.0, 644.0, 645.0, 646.0, 647.0, 648.0, 649.0, 650.0, 651.0, 652.0, 653.0, 654.0, 655.0, 656.0, 657.0, 658.0, 659.0, 660.0, 661.0, 662.0, 663.0, 664.0, 665.0, 666.0, 667.0, 668.0, 669.0, 670.0, 671.0, 672.0, 673.0, 674.0, 675.0, 676.0, 677.0, 678.0, 679.0, 680.0, 681.0, 682.0, 683.0, 684.0, 685.0, 686.0, 687.0, 688.0, 689.0, 690.0, 691.0, 692.0, 693.0, 694.0, 695.0, 696.0, 697.0, 698.0, 699.0, 700.0, 701.0, 702.0, 703.0, 704.0, 705.0, 706.0, 707.0, 708.0, 709.0, 710.0, 711.0, 712.0, 713.0, 714.0, 715.0, 716.0, 717.0, 718.0, 719.0, 720.0, 721.0, 722.0, 723.0, 724.0, 725.0, 726.0, 727.0, 728.0, 729.0, 730.0, 731.0, 732.0, 733.0, 734.0, 735.0, 736.0, 737.0, 738.0, 739.0, 740.0, 741.0, 742.0, 743.0, 744.0, 745.0, 746.0, 747.0, 748.0, 749.0, 750.0, 751.0, 752.0, 753.0, 754.0, 755.0, 756.0, 757.0, 758.0, 759.0, 760.0, 761.0, 762.0, 763.0, 764.0, 765.0, 766.0, 767.0, 768.0, 769.0, 770.0, 771.0, 772.0, 773.0, 774.0, 775.0, 776.0, 777.0, 778.0, 779.0, 780.0, 781.0, 782.0, 783.0, 784.0, 785.0, 786.0, 787.0, 788.0, 789.0, 790.0, 791.0, 792.0, 793.0, 794.0, 795.0, 796.0, 797.0, 798.0, 799.0, 800.0, 801.0, 802.0, 803.0, 804.0, 805.0, 806.0, 807.0, 808.0, 809.0, 810.0, 811.0, 812.0, 813.0, 814.0, 815.0, 816.0, 817.0, 818.0, 819.0, 820.0, 821.0, 822.0, 823.0, 824.0, 825.0, 826.0, 827.0, 828.0, 829.0, 830.0, 831.0, 832.0, 833.0, 834.0, 835.0, 836.0, 837.0, 838.0, 839.0, 840.0, 841.0, 842.0, 843.0, 844.0, 845.0, 846.0, 847.0, 848.0, 849.0, 850.0, 851.0, 852.0, 853.0, 854.0, 855.0, 856.0, 857.0, 858.0, 859.0, 860.0, 861.0, 862.0, 863.0, 864.0, 865.0, 866.0, 868.0, 869.0, 870.0, 871.0, 872.0, 873.0, 874.0, 875.0, 876.0, 877.0, 878.0, 879.0, 880.0, 881.0, 882.0, 883.0, 884.0, 885.0, 886.0, 887.0, 888.0, 889.0, 890.0, 891.0, 892.0, 893.0, 894.0, 895.0, 896.0, 897.0, 898.0, 899.0, 900.0, 901.0, 902.0, 903.0, 904.0, 905.0, 906.0, 907.0, 908.0, 909.0, 910.0, 911.0, 912.0, 913.0, 914.0, 915.0, 916.0, 917.0, 918.0, 919.0, 920.0, 921.0, 922.0, 923.0, 924.0, 925.0, 926.0, 927.0, 928.0, 929.0, 930.0, 931.0, 932.0, 933.0, 934.0, 935.0, 936.0, 937.0, 938.0, 939.0, 940.0, 941.0, 942.0, 943.0, 944.0, 945.0, 946.0, 947.0, 948.0, 949.0, 950.0, 951.0, 952.0, 953.0, 954.0, 955.0, 956.0, 957.0, 958.0, 959.0, 960.0, 961.0, 962.0, 963.0, 964.0, 965.0, 966.0, 967.0, 968.0, 969.0, 970.0, 971.0, 972.0, 973.0, 974.0, 975.0, 976.0, 977.0, 978.0, 979.0, 980.0, 981.0, 982.0, 983.0, 984.0, 985.0, 986.0, 987.0, 988.0, 989.0, 990.0, 991.0, 992.0, 993.0, 994.0, 995.0, 996.0, 997.0, 998.0, 999.0, 1000.0, 1001.0, 1002.0, 1003.0, 1004.0, 1005.0, 1006.0, 1007.0, 1008.0, 1

Table S1. Microbial growth and cell proliferation at 100 μM (mean values and standard deviations)

Ligand	<i>S. aureus</i>	<i>E. coli</i>	<i>C. albicans</i>	HEL 299
H₂L₁	0.3 \pm 0.5	88.9 \pm 8.3	43.6 \pm 6.1	94.5 \pm 7.9
H₂L₂	96.8 \pm 3.5	92.8 \pm 3.1	83.3 \pm 14.4	97.2 \pm 13.2
NaH₂L₄	99.0 \pm 3.5	100.2 \pm 1.0	95.6 \pm 3.2	85.6 \pm 10.2
NaH₂L₅	98.4 \pm 3.0	107.4 \pm 0.9	95.6 \pm 7.5	90.0 \pm 4.9
NaH₂L₆	86.5 \pm 1.9	97.1 \pm 0.7	85.3 \pm 1.6	90.3 \pm 0.8
NaH₂L₇	102.2 \pm 1.9	101.9 \pm 1.3	83.2 \pm 2.7	87.6 \pm 4.9
CIP ¹	0.7 \pm 0.6	0.2 \pm 0.3	n.d. ²	n.d.
FCZ ³	n.d.	n.d.	10.0 \pm 0.6	n.d.
DMSO ⁴	100.0 \pm 2.5	100.0 \pm 4.4	100 \pm 1.5	98.5 \pm 3.1
CP ⁵	n.d.	n.d.	n.d.	9.2 \pm 3.8

¹ CIP, ciprofloxacin at 0.6 μM ; ² n.d., not determined; ³ FCZ, fluconazole at 1.6 μM ; ⁴ DMSO, dimethyl sulfoxide at 0.5%; ⁵ CP, cisplatin at 166.6 μM .

Figure S20: Cisplatin binding interaction with plasmid DNA.



(a) MW, Gene Ruler DNA ladder mix (Thermo Scientific™) in a 1% agarose gel. (b) Electrophoresis analysis of pmaxGFP (Ctrl, 3527 bp) after incubation at 37°C for 2 h with cisplatin (CP) at 500 μM, 100 μM, and 50 μM, and H₂O₂ at 50 mM, 10 mM, 5 mM. Cisplatin binds covalently to the plasmid DNA forming intra-strand crosslinks that cause a shift of the electrophoresis mobility of the open circular form (OC) and the supercoiled form (SC) of the DNA. H₂O₂ does not affect DNA mobility.

Table S2. X-ray crystallographic data for compound $[\text{Ni}(\text{HL6})(\text{H}_2\text{O})_2]_2[\text{Ni}(\text{HL6})(\text{H}_2\text{O})_3]$

Empirical formula	C18 H30 N6 Ni2 O18 S2
Formula weight	800.02
Temperature/K	200.0
Diffractometer/detector	Bruker D8 Venture / PhotonII area detector
Radiation	CuK α (λ = 1.54178)
Crystal system	Monoclinic
Space group	$P2_1/c$
a/Å	9.9485(2)
b/Å	21.3070(5)
c/Å	14.1244(3)
α/°	90
β/°	96.2020(10)
γ/°	90
Volume/Å³	2976.46(11)
Z	4
ρ_{calc} /g·cm⁻³	1.785
μ/mm⁻¹	3.710
F(000)	1648
Θ range for data collection/°	3.77 – 72.56
	-12<h<12
Index ranges	-26<k<26
	-15<l<17
Reflections collected	28031
Unique reflections	5828
Parameters	425
Goodness-of-fit on F²	1.089
Final R indexes [$I \geq 2\sigma(I)$]	R=0.046 wR2=0.131
CCDC Number	2390359

Figure S21 ORTEP representation of $[\text{Ni}(\text{HL6})(\text{H}_2\text{O})_2]_2[\text{Ni}(\text{HL6})(\text{H}_2\text{O})_3]$.

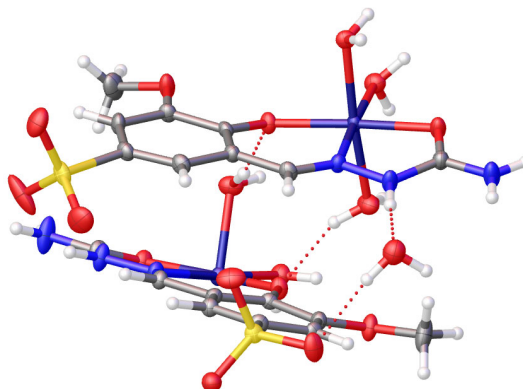
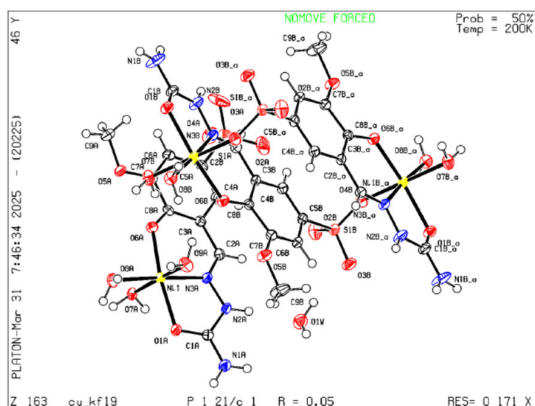


Table S3. X-ray crystallographic data for compound 12

Empirical formula	C ₉ H ₁₅ N ₃ O ₉ S Zn
Formula weight	406.67
Temperature/K	200.0
Diffractometer/detector	Bruker D8 Venture / PhotonII area detector
Radiation	CuK α (λ = 1.54178)
Crystal system	Monoclinic
Space group	<i>P</i> 2 ₁ / <i>c</i>
<i>a</i> /Å	9.4652(2)
<i>b</i> /Å	22.0753(4)
<i>c</i> /Å	7.1489(1)
α /°	90
β /°	99.769(1)
γ /°	90
Volume/Å ³	1472.08(5)
<i>Z</i>	4
ρ_{calc} /g·cm ⁻³	1.835
μ /mm ⁻¹	4.167
<i>F</i> (000)	832
Θ range for data collection/°	4.00 – 70.01
	-11< <i>h</i> <9
Index ranges	-21< <i>k</i> <26
	-8< <i>l</i> <8
Reflections collected	8423
Unique reflections	2718
Parameters	268
Goodness-of-fit on <i>F</i> ²	1.044
Final <i>R</i> indexes [<i>I</i> ≥2 σ (<i>I</i>)]	<i>R</i> =0.030, <i>wR</i> ₂ =0.076
CCDC Number	2435709

Figure S22 ORTEP representation of [Zn(HL6)(H₂O)₂].

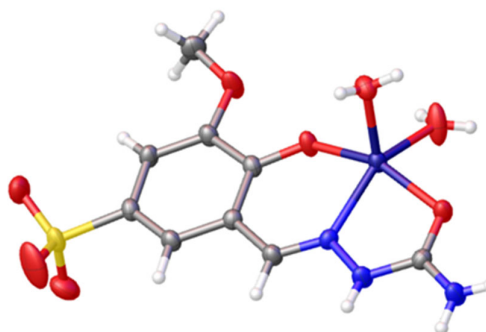
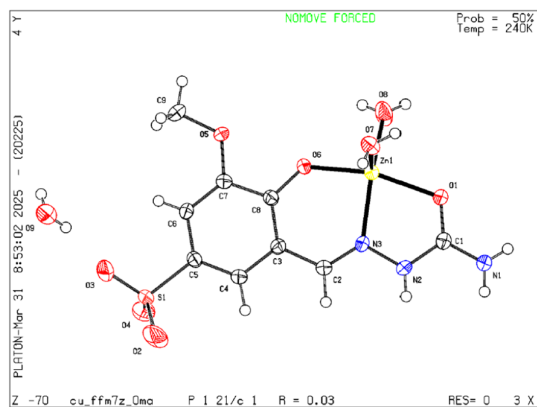


Table S4. X-ray crystallographic data for compound [Cu(HL7)(H₂O)]

Empirical formula	C16 H24 Cu N2 O7 S1
Formula weight	451.97
Temperature/K	200.0
Diffractometer/detector	Bruker D8 Venture / PhotonII area detector
Radiation	CuK α (λ = 1.54178)
Crystal system	Triclinic
Space group	P-1
a/Å	7.4069(4)
b/Å	8.8843(4)
c/Å	15.9868(8)
α/°	101.846(2)
β/°	94.907(2)
γ/°	110.0360(10)
Volume/Å³	953.29(8)
Z	2
ρ_{calc} /g·cm⁻³	1.575
μ/mm⁻¹	3.014
F(000)	470
Θ range for data collection/°	2.87– 72.32
	-9<h<9
Index ranges	-9<k<10
	-19<l<19
Reflections collected	18750
Unique reflections	3753
Parameters	247
Goodness-of-fit on F²	1.075
Final R indexes [I>=2σ (I)]	R=0.032 wR2=0.087
CCDC Number	2435710

Figure S23 ORTEP representation of the head-to-tail dimers [Cu(HL7)(H₂O)]₂ (left) and of the molecular unit [Cu(HL7)(H₂O)]

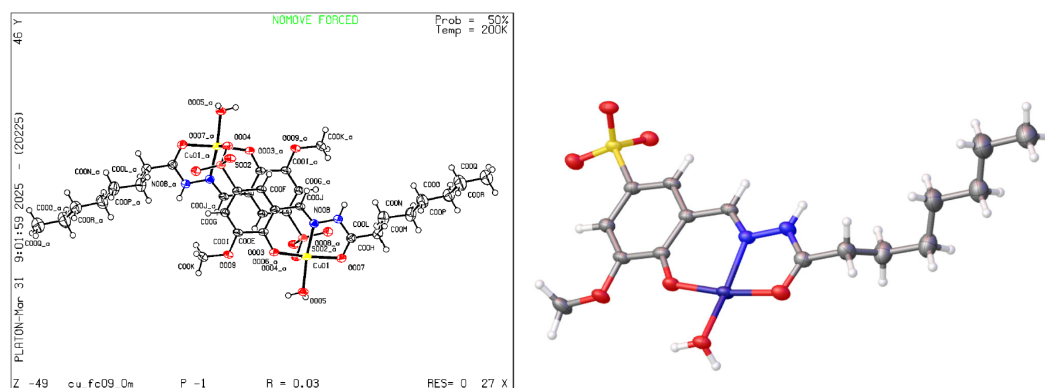


Figure S24. UV-visible spectra for compound **13** (0.25 μ M) dissolved in a 25 mM HEPES/NaCl (0.9%) solution at pH 7.4 over 72 hours.

